IEEE Access
Multidisciplinary ⋮ Rapid Review ⋮ Open Access Journal

Received 28 October 2022, accepted 2 December 2022, date of publication 19 December 2022,
date of current version 29 December 2022.

Digital Object Identifier 10.1109/ACCESS.2022.3230769

RESEARCH ARTICLE

Scenario-Based Fuel Constrained Short-Term Hydrothermal Scheduling

CHITRALEKHA JENA[1], MOUSUMI BASU[2], JOSEP M. GUERRERO[3], (Fellow, IEEE), ABDULLAH ABUSORRAH[4], (Senior Member, IEEE), YUSUF AL-TURKI[4], BASEEM KHAN[5], (Senior Member, IEEE), ANDREA JUSTO[3], AND ARJYADHARA PRADHAN[1]

[1]School of Electrical Engineering, KIIT University, Bhubaneswar, Odisha 751024, India
[2]Department of Power Engineering, Jadavpur University, Kolkata 700032, India
[3]Center for Research on Microgrids (CROM), AAU Energy, Aalborg University, 9220 Aalborg, Denmark
[4]Center of Research Excellence in Renewable Energy and Power Systems, K. A. CARE Energy Research and Innovation Center, Department of Electrical and Computer Engineering, Faculty of Engineering, King Abdulaziz University, Jeddah 21589, Saudi Arabia
[5]Department of Electrical and Computer Engineering, Hawassa University, Hawassa, Ethiopia

Corresponding author: Baseem Khan (baseem.khan04@gmail.com)

ABSTRACT For electric power companies, the economic utilization of existing fossil fuel is currently a primary issue because of the diminishing supply of fossil fuel. Thermal power plants have fuel limitations and contractual restrictions that must be adhered to. As a result, the scenario-based fuel-constrained short-term hydrothermal scheduling problem with renewable energy sources is presented in this paper. The elephant clan optimization (ECO) approach is offered for short-term hydro-thermal scheduling (STHTS) with thermal generators, cascaded hydro, solar PV plants, wind turbine generators (WTG), and pumped storage hydro (PSH) with and without demand side management (DSM) for various scenarios. On a typical test system, the suggested approach is shown to be successful. An analysis of the typical test system's numerical results is compared to those produced via the self-organizing hierarchical particle swarm optimizer with time-varying acceleration coefficients (HPSO-TVAC) and grey wolf algorithms (GWO). The comparison shows that the suggested ECO is capable of providing a better solution.

INDEX TERMS Fuel constraints, solar PV plants, wind turbine generators, cascaded reservoirs, different scenarios, demand side management (DSM), short-term hydrothermal scheduling (STHTS), thermal generators.

NOMENCLATURE

F_C:	Cost function ($).
a_{si}, b_{si}, c_{si}, d_{si}, e_{si}:	Cost coefficients and.
η_{si}, δ_{si}, μ_{si}, λ_{si}, ρ_{si}:	Fuel consumption coefficients of ith thermal generator.
C_{1j}, C_{2j}, C_{3j}, C_{4j}, C_{5j}, C_{6j}:	Power generation co-efficients of jth hydro plant.
Fs_{im}:	During interval m, the fuel delivered to ith thermal.
$Fs_i^{\min}$, $Fs_i^{\max}$:	Lower and upper limits of fuel delivery of ith thermal generator.
F_{Dm}:	The total fuel delivered during period m.
Ih_{jt}, Qh_{jt}:	The inflow rate and rate of discharge of water of jth reservoir at hour t.
$Qh_j^{\min}$, $Qh_j^{\max}$:	Lower and upper rate of discharge of water of jth reservoir.
R_{uj}:	Upstream number of units directly above jth hydro plant.
Sh_{jt}, Vh_{jt}:	Spillage and storage volume of jth reservoir at hour t.
τ_{lj}:	Delay in water transport from reservoir l to j.
$Vh_j^{\min}$, $Vh_j^{\max}$:	Lower and upper volume of storage of jth reservoir.
Vh_{j0}, $Vh_{j\mathrm{M}}$:	Initial and final volume of storage of jth reservoir respectively.

The associate editor coordinating the review of this manuscript and approving it for publication was Lin Wang.

Ps_{it}: At hour t. o/p power of ith thermal generator.

$Ps_i^{\min}$, $Ps_i^{\max}$, UR_i, DR_i: Lowest and highest limits of generation and limits of ramp-up and ramp-down rate for ith thermal generator.

Ph_{jt}: At hour t, o/p power of jth hydro plant.

$Ph_j^{\min}$, $Ph_j^{\max}$: Lower and upper generation limits for jth hydro plant.

Pw_{kt}: At hour t, wind power available of kth WTG.

$Pw_k^{\min}$, $Pw_k^{\max}$: Lower and upper limits of generation for kth WTG.

Pw_{rk}: Rated wind power of kth WTG.

Kd_{wk}: Direct cost co-efficient for kth WTG.

ue_{wk}, oe_{wk}: Penalty and cost of reserve for the kth WTG.

vc_{in}, vc_{out}, vw_r, vw_t: Cut in,cut out, rated speed and forecasted speed of wind respectively.

Ppv_{lt}, Ppv_{rl}: o/p power and rated power output of lth solar plant at hour t.

G_r: Predicted solar irradiation.

T_{ambt}, T_{ref},: Ambient and reference temperature.

α_r: Coefficient of temperature.

Kd_{sl}: Direct cost co-efficient for lth solar plant.

ue_{PVl}, oe_{PVl}: Penalty and reserve cost for lth solar plant.

Pps_{gnt}, Pps_{Pnt}: Power generation and pumping power of nth PSP at hour t.

$Pps_{gn}^{\min}$, $Pps_{gn}^{\max}$: $Pps_{pn}^{\min}$, $Pps_{pn}^{\max}$: minimum and maximum power generation and pumping power limits of nth PSH plant respectively.

$Q_{gnt}\left(Pps_{gnt}\right)$, $Q_{Pnt}\left(Pps_{Pnt}\right)$: Discharge rate and pumping rate of nth PSH plant at hour t.

$V_{res,nt}$: Volume of water in upper reservoir of nth PSH plant at hour t.

$V_{res,n}^{\min}$, $V_{res,n}^{\max}$: Lower and upper limit of upper reservoir storage of nth PSH plant.

$V_{res,n}^{start}$, $V_{res,n}^{end}$: Starting and final specified value of stored water volume in upper reservoir of nth PSH plant.

Vs_{im}: Fuel storage of ith thermal generator in interval m.

$Vs_i^{\min}$, $Vs_i^{\max}$: Lower and upper limit of fuel storage of ith thermal generator.

Vs_i^0: Initial fuel storage of ith thermal generator.

$Incl^{\max}$: At any hour t, maximum augmented demand of power.

$L_{Base,t}$: At hour t, predicted demand of base power demand.

DR_t: At hour t, percentage of predicted based demand participated in DRP.

$Incl_t$, L_{St}: Amount of augmented power demand and transferable power demand at hour t.

T, t,: Scheduling period and time index.

T_{gen}, T_{pump}, T_{change_over}: Set containing all time intervals when PSH plant operated in generation, pumping and idle mode respectively.

t_m: Time period of subinterval m.

M, N_s, N_h,: N_w, N_{PV}, N_{Pump}: Number of subintervals, thermal generators, hydro power plants, WTGs, solar and PSH plants, respectively.

I. INTRODUCTION

Thermal power plants continue to be the primary generators of electric power to this day. There is a fear of a fuel shortage due to the diminishing supply of fossil fuels. For this reason, electric power providers have been obliged to alter their production schedules in response to the fluctuating supply of fuel from their suppliers.

Solar PV and waste-to-gas (WTG) facilities are now being utilized to supply electricity demand without harmful discharges because of growing concerns about climate change and unpolluted energy. Increased uncertainty has resulted from the introduction of climate-driven energy sources such as solar PV plants and WTGs. On the generation schedule, this sort of irregularity presents substantial obstacles that may be solved. This unpredictability may have negative consequences for the grid overall. The integration of PSH plants, which minimize the swings between power production and demand, may mitigate this impact.

A. RELATED WORK

Fuel limits have been taken into account by Trefny and Lee [1] to explain the economic dispatch issue. References [2] and [3] have discussed the scheduling of fuel resources in the energy management field.

Solar PV plants and WTGs have been explored in [4]. Despite the fact that these sources of energy do not produce any pollution or greenhouse gases, they only provide a little quantity of power. Reference [5] describes the combination of thermal generators with renewable energy sources for energy. Here, hydrothermal scheduling, including WTGs, is described [6].

The PSH plant has received a lot of interest around the globe for its ability to store energy [7]. One of the primary functions of PSH plants [8] is to store hydroelectric potential energy, which is a low-cost form of extra electric energy that is available off-peak and may be utilized to generate electricity when demand is high. Evolutionary programming has been considered by Hota et al. [9] to solve hydrothermal scheduling problems for the PSH plant. WTG and PSH

plants have been integrated into hydrothermal scheduling by Helseth et al. [10]. Ma et al. [11] explored the PSH plant for microautonomous systems when it comes to solar energy penetration. Patwal et al. [12] have presented an explanation of hydrothermal scheduling. To overcome short-term hydrothermal scheduling issues, Nguyen et al. [13] used an adaptive cuckoo search approach. Jian et al. [14] used logarithmic-scale mixed-integer linear programming [15] to better describe STHTS. To solve this issue, Yin et al. [15] used crisscross optimization [16]. Kaur et al. [16] used crisscross differential evolution to perform hydrothermal scheduling. Hydrothermal scheduling that takes into account wind infiltration has been detailed in [17]. Sakthivel et al. [18], [19] used quasi-oppositional turbulent water flow-based optimization to perform hydrothermal scheduling.

Demand-side management (DSM) is the most important choice for all energy policy decisions, according to the International Energy Agency's plan. There are several benefits to DSM, including lowering the cost, increasing the security of the system, and much more [20].

For a population-based strategy inspired by elephant behavior and social structure, Jafari et al. [30] created the elephant clan optimization (ECO) algorithm.

Short-term hydrothermal scheduling has been addressed for fuel-limited thermal generators, cascaded reservoir hydropower facilities, solar PV plants, WTGs, and PSH plants with and without DSM.

B. RESEARCH GAP

Hydrothermal scheduling problems for different scenarios have not been considered in any of the above papers. Different restrictions on thermal and hydropower-producing capacities for both thermal and hydro units, as well as ramp rates for thermal generators, were also not considered. Fuel restrictions and thermal generator ramp rate limits haven't been taken into account.

In our estimates, we account for solar PV and WTGs. Thermal and hydropower-producing capacity limitations for both thermal and hydro units, as well as thermal generator ramp rates, are the primary constraints.

The problem of STHTS is solved with and without DSM in three distinct conditions using ECO. Comparisons have been made between the test results and those obtained using the HPSO-TVAC (self-organizing hierarchical particle swarm optimizer with time-varying acceleration coefficients) and the Grey Wolf Optimization (GWO). The comparison shows that the suggested ECO is a higher-quality alternative. Fig. 1 shows the schematic representation of the proposed problem formulation.

This manuscript's most significant features are as follows:

- Hydrothermal scheduling problems for different scenarios have been considered.
- Fuel restrictions and thermal generator ramp rate limits were taken into account.
- With or without DSM, the problem is solved.
- Elephant clan optimization has been employed to solve this problem.

II. FORMULATION OF PROBLEM

The primary goal of STHTS is to incorporate a combination of solar PV, WTG, and PSH plants with DSM for different scenarios in order to minimize both thermal generators' fuel costs as well as the costs of WTGs and solar plants while taking advantage of all hydro resources that are available during the scheduling horizon.

$$\begin{aligned}\text{Minimize } F_c = \sum_{t=1}^{\mathrm{T}} \Bigg[& \sum_{i=1}^{\mathrm{N}_s} \{fs_{it}(\mathrm{P}s_{it})\} \\ & + \sum_{k=1}^{\mathrm{N}_W} \{\mathrm{K}d_{wk} \times \mathrm{P}w_{kt} + Oe_{wkt}(\mathrm{P}w_{kt}) + Ue_{wkt}(\mathrm{P}w_{kt})\} \\ & + \sum_{l=1}^{\mathrm{N}_{PV}} \{\mathrm{K}d_{sl} \times \mathrm{P}pv_{lt} + Oe_{PVlt}(\mathrm{P}pv_{lt}) + Ue_{PVlt}(\mathrm{P}pv_{lt})\} \Bigg] \end{aligned} \tag{1}$$

When the valve-point impact [29] is taken into account, the cost function of fuel for the i-th generator at hour t is affirmed as

$$\begin{aligned} fs_{it}(\mathrm{P}s_{it}) = a_{si} + b_{si}\mathrm{P}s_{it} + c_{si}\mathrm{P}s_{it}^2 \\ + \left| d_{si} \times \sin\left\{ e_{si} \times \left(\mathrm{P}s_i^{\min} - \mathrm{P}s_{it} \right) \right\} \right| \end{aligned} \tag{2}$$

The costs of overestimating and underestimating dispatchable wind power [22], as well as the costs of reserve and penalty, are confirmed.

$$Oe_{wkt}(\mathrm{P}w_{kt}) = e_{wk} \times \int_{\mathrm{P}w_{kt}^{\min}}^{\mathrm{P}w_{kt}} (\mathrm{P}w_{kt} - y) \times fw(y)\, dy \tag{3}$$

$$Ue_{wkt}(\mathrm{P}w_{kt}) = ue_{wk} \times \int_{\mathrm{P}w_{kt}}^{\mathrm{P}w_{kt}^{\max}} (y - \mathrm{P}w_{kt}) \times fw(y)\, dy \tag{4}$$

Due to overestimation and underestimation of dispatchable solar power, the reserve and penalty costs [23] are computed as follows:

$$Oe_{PVlt}(\mathrm{P}pv_{lt}) = oe_{PVl} \times \int_{\mathrm{P}pv_{lt}^{\min}}^{\mathrm{P}pv_{lt}} (\mathrm{P}pv_{lt} - x) \times fpv(x)\, dx \tag{5}$$

$$Ue_{PVlt}(\mathrm{P}pv_{lt}) = ue_{PVl} \times \int_{\mathrm{P}pv_{lt}}^{\mathrm{P}pv_{lt}^{\max}} (x - \mathrm{P}pv_{lt}) \times fpv(x)\, dx \tag{6}$$

subject to

A. POWER BALANCE CONSTRAINTS

$$\begin{aligned} \sum_{i=1}^{\mathrm{N}_s} \mathrm{P}s_{it} + \sum_{j=1}^{\mathrm{N}_h} \mathrm{P}h_{jt} + \sum_{k=1}^{\mathrm{N}_W} \mathrm{P}w_{kt} + \sum_{l=1}^{\mathrm{N}_{PV}} \mathrm{P}pv_{lt} + \sum_{n=1}^{\mathrm{N}_{pump}} \mathrm{P}ps_{gnt} \\ = (1 - DR_t) \times L_{Base,t} + L_{St} + \mathrm{P}_{Lt}, t \in \mathrm{T}_{gen} \end{aligned} \tag{7}$$

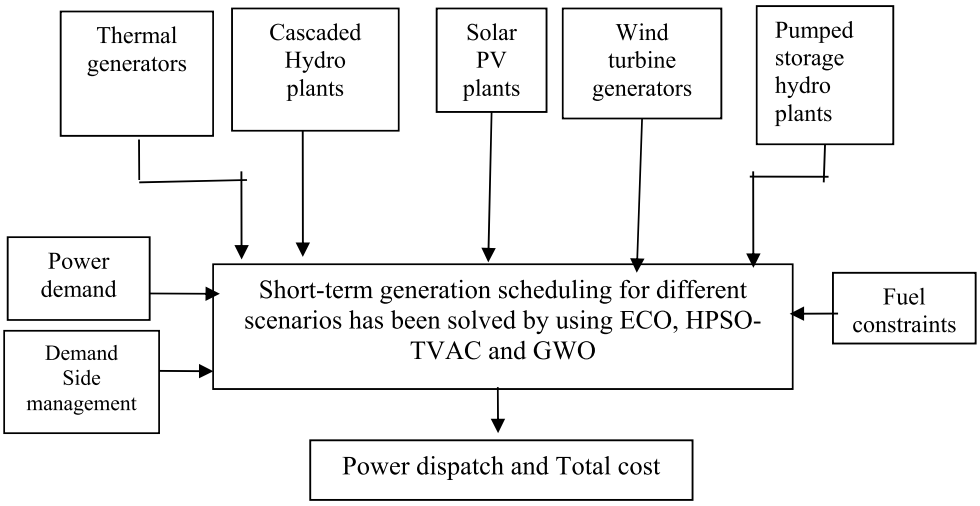

FIGURE 1. Schematic representation of the overall proposed problem formulation.

$$\sum_{i=1}^{N_s} Ps_{it} + \sum_{j=1}^{N_h} Ph_{jt} + \sum_{k=1}^{N_W} Pw_{kt} + \sum_{l=1}^{N_{PV}} Ppv_{lt} - \sum_{n=1}^{N_{pump}} Pps_{Pnt} = (1 - DR_t) \times L_{Base,t} + L_{St} + P_{Lt}, t \in T_{pump} \quad (8)$$

$$\sum_{i=1}^{N_s} Ps_{it} + \sum_{j=1}^{N_h} Ph_{jt} + \sum_{k=1}^{N_W} Pw_{kt} + \sum_{l=1}^{N_{PV}} Ppv_{lt} = (1 - DR_t) \times L_{Base,t} + L_{St} + P_{Lt}, t \in T_{change\_over} \quad (9)$$

Taking the assumption that, when power demand is curtailed due to DRP, Lst = 0 at that time While the demand for power is shifted to the base demand, it is not curtailed during that time.

A hydroelectric plant's power generation is determined by the rate of discharge of water and the amount of water stored in the reservoir.

$$Ph_{jt} = C_{1j}Vh_{jt}^2 + C_{2j}Qh_{jt}^2 + C_{3j}Vh_{jt}Qh_{jt} + C_{4j}Vh_{jt} + C_{5j}Qh_{jt} + C_{6j}, \quad j \in N_h \; vt \in T \quad (10)$$

B. WIND POWER MODEL

Depending on the wind speed, the WTG's power output might vary greatly. Power output and wind speed are non-linearly connected by using operational factors such as the WTG's cut-in speed and rated speed as well as its cut-out speed [24]. For a given wind speed, the kth WTG output power at t hours is given as,

$$\begin{aligned} P_{wkt} &= 0, \quad \text{for } vw_t < vc_{in} \text{ and } vw_t > vc_{out} \\ P_{wkt} &= \left(A_w + B_w vw_t + C_w vw_t^2\right) P_{wrk} \quad \text{for } vc_{in} \le vw_t < vw_r \\ P_{wkt} &= P_{wrk}, \quad \text{for } vw_r \le vw_t \le vc_{out} \end{aligned} \quad (11)$$

Constants A_w, B_w, and C_w are function of vc_{in} and vw_r and are calculated by using the following equations:

$$A_w = \frac{1}{(vc_{in} - vw_r)^2}\left[vc_{in}(vc_{in} + vw_r) - 4vc_{in}vw_r\frac{(vc_{in} - vw_r)^3}{2vw_r}\right] \quad (12)$$

$$B_w = \frac{1}{(vc_{in} - vw_r)^2}\left[2 - 4\frac{\left(\frac{4}{vc_{in}} + vw_r\right)^3}{2vw_r}\right] \quad (13)$$

$$C_w = \frac{1}{(vc_{in} - vw_r)^2}\left[4(vc_{in} + vw_r) + \frac{(vc_{in} + vw_r)^3 - (3vc_{in} + vw_r)}{2vw_r}\right] \quad (14)$$

C. MODEL OF SOLAR POWER

The power output [25] of the lth solar plant at hour t is stated as

$$Ppv_{lt} = Ppv_{rl} \times \left[1 + \alpha_r \times \left(T_{ref} - T_{amb,t}\right)\right] \times \frac{G_r}{1000} \quad (15)$$

D. CONSTRAINTS FOR DELIVERY OF FUEL

Over the scheduling horizon, the total fuel supplied will equal the total fuel given to all generators.

$$\sum_{i=1}^{N_s} Fs_{im} - F_{Dm} = 0, \quad m \in M \quad (16)$$

E. CONSTRAINTS FOR FUEL STORAGE

At the beginning of each period, the amount of fuel in the thermal generators is divided by the amount of fuel given to those generators minus the amount of fuel consumed by those generators.

$$Vs_{im} = Vs_{i(m-1)} + Fs_{im} - \sum_{t=1}^{t_m}\left[\eta_{si} + \delta_{si}Ps_{it} + \mu_{si}Ps_{it}^2 + \left|\lambda_{si}\sin\left\{\rho_{si}\left(Ps_i^{\min} - Ps_{it}\right)\right\}\right|\right], \quad i \in N_s, \; m \in M \quad (17)$$

F. LIMITS OF FUEL DELIVERY

Each thermal generator's fuel supply is within its $Fs^{\min}$ and maximum limits $Fs^{\max}$ at all times.

$$Fs_i^{\min} \le Fs_{im} \le Fs_i^{\max}, \quad i \in \mathrm{N}_s,\ m \in \mathrm{M} \tag{18}$$

G. LIMITS OF FUEL STORAGE

Each generator's capacity for fuel storage must remain within its minimum $Vs^{\min}$ and maximum limits $Vs^{\max}$ at each interval.

$$Vs_i^{\min} \le Vs_{im} \le Vs_i^{\max}, \quad i \in \mathrm{N}_s,\ m \in \mathrm{M} \tag{19}$$

H. PSH PLANT CONSTRAINTS

Pumping of water is done from the lower to the higher reservoir at the PSH plant during off-peak hours in order to generate power during periods of high demand. As a result of the PSH plant's physical limitations, it must be shut down for an hour each time it switches from producing to pumping mode, and this period is referred to as the ''changeover time.''

$$V_{res,n(t+1)} = V_{res,nt} + Q_{Pnt}\left(\mathrm{P}sp_{Pnt}\right), \quad n \in \mathrm{N}_{pump},\ t \in \mathrm{T}_{pump} \tag{20}$$

$$V_{res,n(t+1)} = V_{res,nt} - Q_{gnt}\left(\mathrm{P}sp_{gnt}\right), \quad n \in \mathrm{N}_{pump},\ t \in \mathrm{T}_{gen} \tag{21}$$

$$V_{res,n(t+1)} = V_{res,nt}, \quad n \in \mathrm{N}_{pump} \text{ and } t \in \mathrm{T}_{change\_over} \tag{22}$$

$$\mathrm{P}sp_{gn}^{\min} \le \mathrm{P}sp_{gnt} \le \mathrm{P}sp_{gn}^{\max}, \quad n \in \mathrm{N}_{pump},\ t \in \mathrm{T}_{gen} \tag{23}$$

$$\mathrm{P}sp_{Pn}^{\min} \le \mathrm{P}sp_{Pnt} \le \mathrm{P}sp_{Pn}^{\max}, \quad n \in \mathrm{N}_{pump},\ t \in \mathrm{T}_{pump} \tag{24}$$

$$V_{res,n}^{\min} \le V_{res,nt} \le V_{res,n}^{\max}, \quad n \in \mathrm{N}_{pump},\ t \in \mathrm{T} \tag{25}$$

The initial and final volumes of water in the upper reservoir of the PSH plant are presumed to be similar.

$$V_{res,n0} = V_{res,n\mathrm{T}} = V_{res,n}^{start} = V_{res,n}^{end} \tag{26}$$

I. GENERATION LIMITS

$$\mathrm{P}h_j^{\min} \le \mathrm{P}h_{jt} \le \mathrm{P}h_j^{\max} \quad j \in \mathrm{N}_h\ t \in \mathrm{T} \tag{27}$$

$$\mathrm{P}s_i^{\min} \le \mathrm{P}s_{it} \le \mathrm{P}s_i^{\max} \quad i \in \mathrm{N}_s,\ t \in \mathrm{T} \tag{28}$$

J. LIMITS OF RAMP RATE OF THERMAL GENERATORS

$$\begin{aligned} \mathrm{P}s_{it} - \mathrm{P}s_{i(t-1)} &\le UR_i, \quad i \in \mathrm{N}_s,\ t \in \mathrm{T} \\ \mathrm{P}s_{i(t-1)} - \mathrm{P}s_{it} &\le DR_i, \quad i \in \mathrm{N}_s,\ t \in \mathrm{T} \end{aligned} \tag{29}$$

K. CONSTRAINTS FOR HYDRAULIC NETWORK

Hydraulic restrictions include water balance formulas for each hydroelectric facility, as well as storage and discharge goals for reservoirs. These boundaries are set by the hydro system's many functions and the physical restrictions of the reservoirs and plants that support them. Constraints include:

(a) Physical limits on water reservoir storage volumes and rate of discharge,

$$Vh_j^{\min} \le Vh_{jt} \le Vh_j^{\max} \quad j \in \mathrm{N}_h,\ t \in \mathrm{T} \tag{30}$$

$$Qh_j^{\min} \le Qh_{jt} \le Qh_j^{\max} \quad j \in \mathrm{N}_h,\ t \in \mathrm{T} \tag{31}$$

(b) Continuity equation for hydro reservoir system

$$\begin{aligned} Vh_{j(t+1)} = {} & Vh_{jt} + \mathrm{I}h_{jt} - Qh_{jt} - Sh_{jt} \\ & + \sum_{l=1}^{R_{uj}} \left(Qh_{l(t-\tau_{lj})} + Sh_{l(t-\tau_{lj})}\right), \\ & j \in \mathrm{N}_h, \quad t \in \mathrm{T} \end{aligned} \tag{32}$$

L. DEMAND SIDE MANAGEMENT

As a result of demand side management (DSM), there are several benefits, such as decreasing costs, improving power system security, and so on [20]. Demand response programs (DRP), tactical conservation, etc. are some examples of DSM initiatives. A time-of-use (TOU) program [21] combined with DRP can shift demand from peak hours to off-peak hours while still maintaining the overall level of demand for electricity. The result is a flattening of the electricity demand curve. The TOU program is designated by equation (33) and constrained by equations (34)–(37).

$$L_t = (1 - DR_t) \times L_{Base,t} + L_{St} \tag{33}$$

$$\sum_{t=1}^{\mathrm{T}} L_{St} = \sum_{t=1}^{\mathrm{T}} DR_t \times L_{Base,t} \tag{34}$$

$$L_{Incl_t} = Incl_t \times L_{Base,t} \tag{35}$$

$$DR_t \le DR^{\max}, \quad t \in \mathrm{T} \tag{36}$$

$$Incl_t \le Incl^{\max}, \quad t \in \mathrm{T} \tag{37}$$

III. ELEPHANT CLAN OPTIMIZATION

Elephant clan optimization (ECO) has been developed by Jafari et al. [30]. A populace-driven method, ECO, was inspired by elephants' behavior and societal structure. Unlike humans, elephants have a long-term memory and a strong capacity to learn new things. Needing water, food, and rest, elephants are known to travel great distances. As the group's leader, it's up to the materfamilias to guide them to their destination. The materfamilias may identify the route to water and food supplies by drawing on their memories and experiences. The male elephants that are growing and maturing out of their group are now living on their own or with other male elephants. The male elephant joins the family group just for mating and competition, and to encourage the birth of offspring from stronger generations. Only two parameters can be changed in the ECO algorithm.

In the ECO algorithm, there are many family clans and a single male clan. The eldest female elephant, known as materfamilias, is in charge of each family clan, which consists of many female elephants and their calves. The male elephants can stay in the male clan when they're well-advanced adults. Those that are stupid will be left out of the optimization process, so they will have to survive on their own. Optimizing each clan's population size has been a constant consideration. As a result, the number of elephants that have perished or left their family group is the same as the number of elephants that were born into the group.

As a result of this knowledge, the algorithm's four key operators have become more familiar.

(i) The family clan update operator takes into account the best elephant in each group in order to keep the family informed. Global search is boosted by the mobility of these elephants during the optimization process.

(ii) It is necessary to minimize the amplitude of current male elephants to update their positions in the male clan throughout the optimization procedure. In the beginning, the capacity to hunt globally was aided by the mobility of male elephants. To improve exploitation, the search is limited to locations around the current location as the iteration progresses.

(iii) The generator operator uses the community's best members to produce better and fresher members. This operator expands the community's options for a suitable setting, which aids in local search.

(iv) The male clan's members are turned upside down via the substitution operator. In the optimization process, mature male elephants were used to update and improve the elephant placements.

A solution $\left(\mathrm{X} = \left\lfloor x_1, x_2, \ldots, x_j, \ldots, x_{\mathrm{N}} \right\rfloor\right)$ in the M-dimensional search space is symbolized by an elephant, and objective function is an elephant's fitness value, which is expressed as f (M). ECO algorithm's stages are summarised:

Step 1: Two variable parameters, α and β, which are initialised with the number of elephants ($\mathrm{N_P}$) and the number of clans (N_c), balance the algorithm's exploration and exploitation capabilities.

Step 2: A family clan and a male clan make up each of the *Nc* clans that are created at random from the overall population.

Step 3: In the group of elephants, the fitness function determines each individual's fitness value.

Step 4: Members of the same family clan are ranked according to their fitness, and the materfamilias of each family is held in high regard.

Step 5: Members of a family clan shift in response to their materfamilias' place in the clan structure:

Where $\boldsymbol{xFCiEmj}$ and $\boldsymbol{xFCiMj}$ are the variables of elephant m an the mater familias in family clan I respectively. Furthermore, it signifies the present iteration, $\boldsymbol{\alpha}$ is the scaling factor, which controls exploration and exploitation balancing. r is a random number between 0 and 1.

Step 6: Every family's materfamilias moves in accordance with the collective wisdom of its members.

Where $x_{best,j}$ is the j^{th} variable of the best experience acquired by the whole populace, β is a scaling factor, controlling exploration and exploitation balancing.

Step 7: When the elephants finally mate, the best female elephants are chosen as calves and used to determine the elephants' new positions.

Step 8: Every clan's worst calf has been culled because it has died or been killed by its rivals.

Step 9: When they reach maturity, male calves separate from their mothers' herds. With other male members of the male clan, they either live alone or in a group. In this method, all the elephant calves in each family are randomly selected to become adult male elephants.

Step 10: The male elephants of the male clan are the ones that make their own decisions and wander about the search area without having a specific aim in mind.

in where $x_{\mathrm{MC},E_m,j}$ indicates the j th elephant m in the male clan's variable list, and r is a random value between -1 and 1, dictating the random movement of each component. Aside from that, the values $x_j^{\max}$ and $x_j^{\min}$ represent the high and low positions of the j th variable, respectively.

A parameter called p restricts the movement of male elephants in the search space, and it decreases as the optimization progresses. This parameter is stated as follows: ''C is a factor that affects the pace at which aimless members travel in a region around the member's current location and is chosen based on the optimal operating mode.'' In this case, 0.5 is the consistent value for the coefficient. It is the current iterative number, but the maximum iterative number is it_{max}.

Step 11: For mating and reproducing, only the finest elephants are maintained in the male clan, where their new rank is decided.

Step 12: It is the weakest member of each male elephant's family group that is updated when a grown elephant departs from his family group.

where $\mathrm{X}_{\mathrm{MC},worst}$ is the feeblest elephant in the male clan, and $\mathrm{X}_{FC_i,\mathrm{GM}}$ is the matured male elephant in family clan i.

Step 13: A calf is born when one of the best male elephants meets one of the best female elephants from each familial group. Fresh calves, taken from the familial clans, have taken their place. The following is a list of parents that are used to produce the young calves:

where $x_{FC_i,calf,j}$ denotes variable j of a new born calf in clan i and $x_{FC_i,Rf,j}$ and $x_{\mathrm{M}c,Rm,j}$ are variable j of a random female of clan i and a random male of the best elephants of the male clan, respectively

Step 14: Every elephant family's new arrivals are plotted out.

Step 15: A maximum of 14 iterations is reached by repeating steps 4–14, and the program then delivers the best experience gained during optimization.

Fig. 2 shows the flowchart of ECO algorithm.

IV. NUMERICAL RESULTS AND DISCUSSION

The test system was solved in three distinct methods, both with and without DSM, using the elephant clan optimization (ECO) approach. The efficacy of the suggested ECO has been matched to that of HPSO-TVAC [31] and grey wolf optimization [32].

To simulate the projected Eco, HPSO-TVAC, and GWO, MATLAB (version 8.1.0.504.R2013a) is used in a 64-bit system with an Intel Core (TM) i7-4770 CPU at 3.66 GHz and 16 GB of RAM.

ECO, HPSO-TVAC, and GWO are used to resolve the issue. In case of ECO, parameters are taken as $\mathrm{N_P} = 100$,

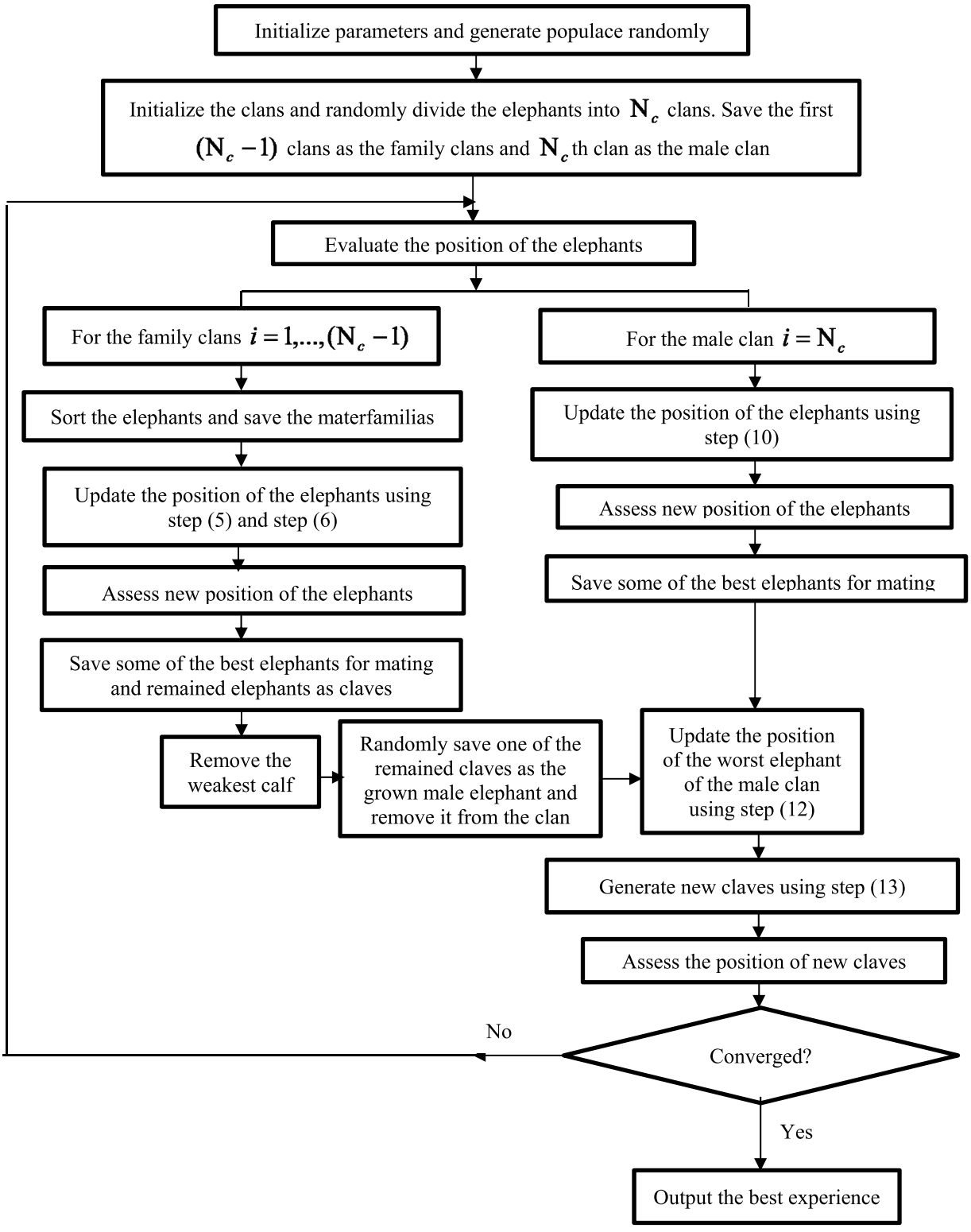

FIGURE 2. Flowchart of ECO algorithm.

$N_c = 10$, $\alpha = \beta = 2$. In HPSO-TVAC, parameters taken are $N_P = 100$, $w_{max} = 0.25$, $w_{min} = 0.05$, $c_{1i} = 2.5$, $c_{1f} = 0.2$ and $c_{2i} = 0.2$, $c_{1f} = 2.5$. For the purposes of GWO, a wolf population of 100 is considered adequate.300 is the maximum number of iterations for each of the three approaches.

TABLE 1. Limits of Generation, ramp rate limits, cost coefficients of fuel and initial storage of fuel of coal-burnt thermal units.

Unit	Ps^{min} MW	Ps^{max} MW	a_s \$/h	b_s \$/MWh	c_s \$/ MW^2h	d_s \$/h	e_s rad/MW	UR MW/h	DR MW/h	Vs^0 ton
1	36	114	94.705	6.73	0.00690	100	0.084	40	40	200
2	36	114	94.705	6.73	0.00690	100	0.084	40	40	200
3	60	120	309.540	7.07	0.02028	100	0.084	40	40	200
4	80	190	369.030	8.18	0.00942	150	0.063	60	60	200
5	47	97	148.890	5.35	0.01140	120	0.077	30	30	200
6	68	140	222.330	8.05	0.01142	100	0.084	50	50	200
7	110	300	287.710	8.03	0.00357	200	0.042	80	80	500
8	135	300	391.980	6.99	0.00492	200	0.042	80	80	500
9	135	300	455.760	6.60	0.00573	200	0.042	80	80	500
10	130	300	722.820	12.90	0.00605	200	0.042	80	80	500

TABLE 2. Consumption of fuel coefficients, fuel delivery and limits of fuel storage of coal-burnt thermal units.

Unit	η_s ton/h	δ_s ton/MWh	μ_s ton/$(MW)^2$h	λ_s ton/h	ρ_s rad/MW	Fs^{min} ton	Fs^{max} ton	Vs^{min} ton	Vs^{max} ton
1	0.83612	0.066889	0.00026756	1.0	0.15	0	100	0	1000
2	0.83612	0.066889	0.00026756	1.0	0.15	0	100	0	1000
3	2.00669	0.060200	0.00010033	1.5	0.10	0	100	0	1000
4	3.34448	0.070230	0.00004013	2.0	0.09	0	100	0	1000
5	0.83612	0.066889	0.00026756	1.0	0.15	0	100	0	1000
6	2.00660	0.060200	0.00010033	1.5	0.10	0	100	0	1000
7	4.01338	0.073578	0.00013378	2.5	0.07	0	200	0	2000
8	1.33779	0.060200	0.00005017	3.0	0.05	0	200	0	2000
9	1.33779	0.060200	0.00005017	3.0	0.05	0	200	0	2000
10	1.33779	0.060200	0.00005017	3.0	0.05	0	200	0	2000

A. TEST SYSTEM DESCRIPTION

The testing system takes into consideration ten coal-fired thermal generators, one equivalent WTG, one equivalent solar PV plant, and a multi-chained reservoir hydroelectric facility.

Each day is divided into 24 periods, each holding an hour of scheduling time. There are three ways to tackle the problem. There is 0.9 times as much power demand on day one as there is on day two, as seen in Table 3. Table 3 shows that the second day's power demand is the same as the first day. Table 3 shows that the third day's power demand is 1.1 times greater than the third day's power demand shown in Table 3.

Coal-burning thermal reactors' ramp rate restrictions and valve point effects are taken into account. According to [25], hydro plants' system specifications are given. Tables 1 and 2 contain all the data you'll need concerning coal-fired power stations, including cost and coefficients of coal consumption, fuel supply and storage constraints, and initial fuel storage. Table 3 displays the temperature over the course of a 24-hour period. Table 4 shows the energy that was delivered on schedule and in accordance with the plan. Numbers two and three represent the lowest and highest expected limits for solar irradiation and wind velocity, respectively. The rating of WTG is $P_{wr} = 150$ MW. Cut in, cut out and rated speed of wind are $vc_{in} = 4$m/sec, $vc_{out} = 25$m/s and $vw_r = 15$m/s respectively. Direct cost coefficient (Kd_w) for WTG is chosen 7. The reserve cost (oe_w) and penalty cost (ue_w) for WTG are chosen as 2 and 1 respectively. Solar plant rating is $P_{PVr} = 175$ MW. Direct cost coefficient (Kd_s) of solar plant is chosen 6. Reserve cost (oe_{PV}) and penalty cost (ue_{PV}) is taken as 2 and 1 respectively. T (T_{ref}) is assumed as 25^0C and coefficient of temperature (α_r) is chosen as -0.0025/Kelvin. During DSM 10% of 15^{th}, 16^{th} and 17^{th} hour load is shifted to 3^{rd}, 4^{th} and 5^{th} hour. PSH plant has the below characteristics:

Generating mode

Q_{ght} is positive while generating, Ps_{ght} is positive and $0 \leq Ps_{ght} \leq 100$MW, $Q_{ght}\left(Ps_{ght}\right) = 50 + 2Ps_{ght}$ acre-ft/hr.

Pumping mode

Q_{pht} is negative while pumping, Ps_{pht} is negative and $-100MW < Ps_{pht} \leq 0MW$, $Q_{pht}\left(Ps_{pht}\right) = -200$ acre-ft/h with $Ps_{pht} = -100$ MW.

Operating restrictions: While pumping, the PSH is only allowed to run at a maximum of 100 MW. The reservoir's capacity is set at 3000 acre-feet, and it must remain at this level for the duration of the 24-hour period.

TABLE 3. Hourly temperature and power demand.

Hour	L_{Base} (MW)	Temperature (°C)	Hour	L_{Base} (MW)	Temperature (°C)	Hour	L_{Base} (MW)	Temperature (°C)
1	1530	23	9	1900	27	17	2080	26
2	1570	23	10	1990	28	18	1920	25
3	1605	24	11	2050	29	19	2020	24
4	1610	25	12	2140	29	20	1980	24
5	1680	25	13	2200	29	21	1930	24
6	1740	25	14	2150	28	22	1840	24
7	1800	26	15	2250	28	23	1760	23
8	1860	27	16	2100	27	24	1690	23

TABLE 4. Fuel delivered within period of scheduling.

Interval	Duration (h)	Fuel delivered F_D(ton)
1	4	300
2	4	400
3	4	600
4	4	600
5	4	400
6	4	300

1) SIMULATION RESULTS

Table 1 contains data for 10 thermal generating units, including generation limit, ramp-up rate and ramp-down rate limit, fuel cost co-efficient and initial storage of fuel.

Table 2 shows data on the coefficients of fuel consumption, limits of fuel delivery, and limits of fuel storage for coal-burning thermal units. It is seen that the initial fuel delivery and initial fuel storage are both "0."

Table 3 displays the 24-hour base load demand along with the hourly temperature. The temperature rises with the hour and reaches its peak between the tenth and fifteenth hours. At the 13th hour, the base load demand is at its peak.

Table 4 depicts the amount of fuel delivered over six four-hour intervals. The maximum fuel delivered is at the third and fourth intervals.

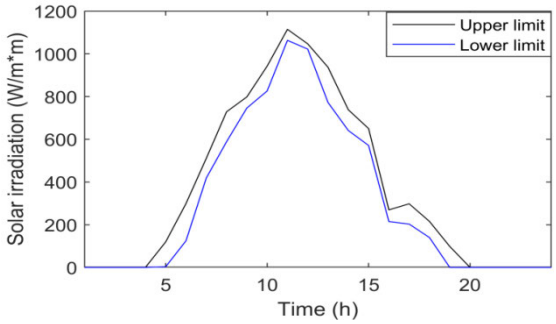

FIGURE 3. The lower and upper forecast limits of solar irradiation.

Figure 3 shows the variation of solar irradiation in W/m^2 with time in hours. The black, bold line shows the upper limit, and the blue line shows the lower forecast limits of solar irradiation. The maximum upper limit is 1115 W/m^2, whereas the maximum lower limit is 1063 W/m^2.

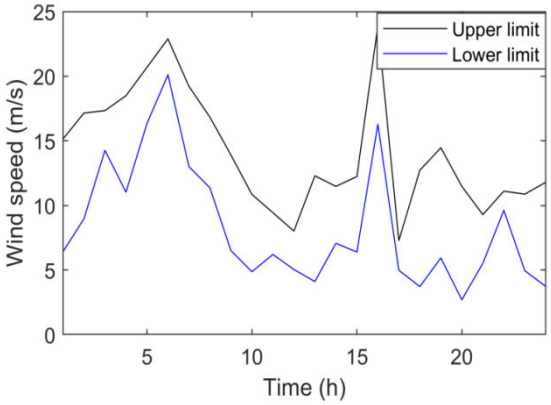

FIGURE 4. The Lower and upper forecast limits of wind speed.

Figure 4 depicts the relationship between wind speed in m/s and time in hours. The black, bold line shows the upper limit, while the blue line shows the lower forecast limits of solar irradiation. The maximum upper limit is 23.90399 m/s, whereas the maximum lower limit is 20.1123 m/s.

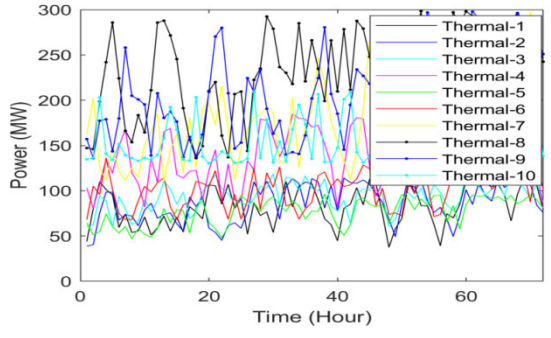

FIGURE 5. Power generation obtained from thermal generators with DSM and fuel constraints using ECO.

Figure 5 shows the power generation received from 10 thermal units with demand-side management and fuel limits corresponding to the best cost using ECO. Here the time span is 72 hours. In the first 24 hours, the power demand was 0.9 times higher than the demand given in Table 2. From

the 25th to the 48th hour, the power demand is the same as in Table 3. From the 49th to the 72nd hour, the power demand is 1.1 times what it is in Table 2.

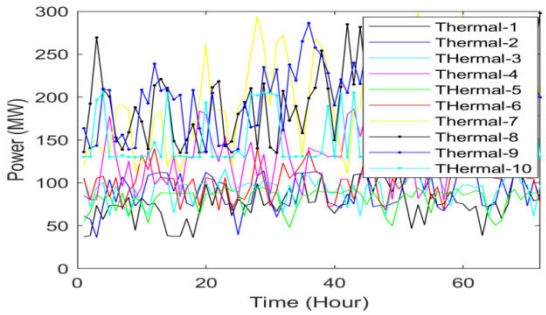

FIGURE 6. Power Generation received from thermal units with DSM using ECO.

The graph in Fig. 6 shows the variation of power generated in MW received from ten thermal units with respect to time in an hour, considering DSM using ECO without fuel constraints. The time required is 72 hours.

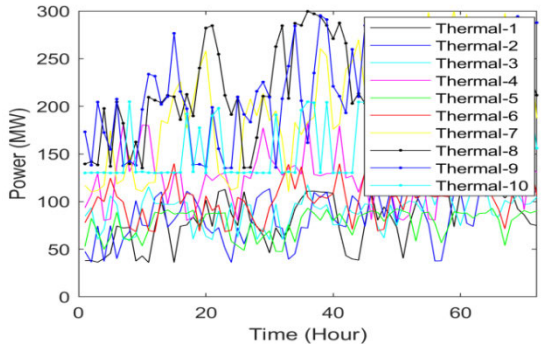

FIGURE 7. Power Generation received from thermal units without DSM using ECO.

Figure 7 shows the variation of power generated in MW received from ten thermal units without DSM and without fuel constraints using ECO with respect to time in an hour. The time span used in this case is 72 hours.

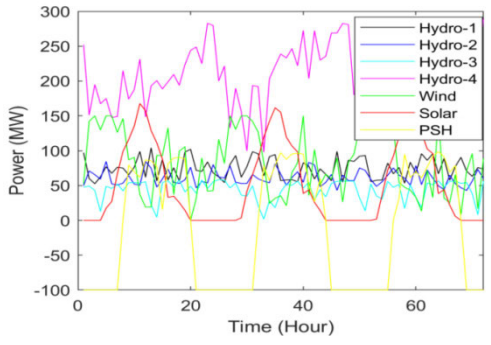

FIGURE 8. Power Generation received from different plants with DSM and fuel constraints using ECO.

Figure 8 shows the power generation from different plants with DSM and fuel constraints using ECO. With ECO, the generation of power is obtained from four hydropower plants: one WTG, one solar, and one PSH plant, with DSM considering fuel constraints corresponding to the best cost over a span of 72 hours.

Figure 9 depicts the variation of power generation in MW with time in hours from four hydropower plants: one WTG, one solar plant, and one PSH plant, with DSM corresponding to the best cost using ECO and without fuel constraints over a 72-hour period.

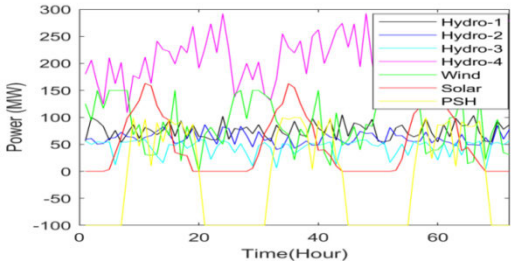

FIGURE 9. Power Generation received from different plants with DSM using ECO.

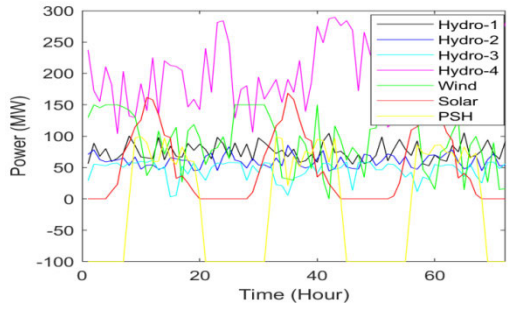

FIGURE 10. Power Generation received from different plants without DSM using ECO.

Figure 10 shows the variation of power generation in MW with time (in hours) obtained from four hydropower plants, one WTG, one solar plant, and one PSH plant, corresponding to the best cost using ECO without DSM and without fuel constraints for a time span of 72 hr.

Figure 11 depicts the variation of power generation in MW with time (in hours), corresponding to the best cost obtained from ten thermal generating units using HPSO-TVAC with DSM and fuel constraints over a 72-hour period.

Figure 12 depicts the variation of power generation in MW with time (in hours), corresponding to the best cost obtained from ten thermal generating units using HPSO-TVAC with DSM and no fuel constraints over a 72-hour period.

Figure 13 depicts the variation of power generation in MW with time (in hours), which corresponds to the best cost obtained from ten thermal generating units using HPSO-TVAC without DSM and without fuel constraints over a 72-hour period.

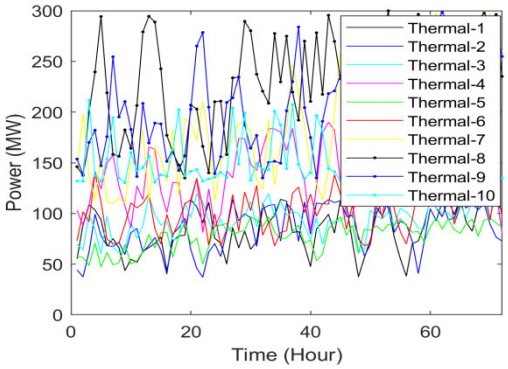

FIGURE 11. Power Generation received from thermal unit with DSM and fuel constraints using HPSO-TVAC.

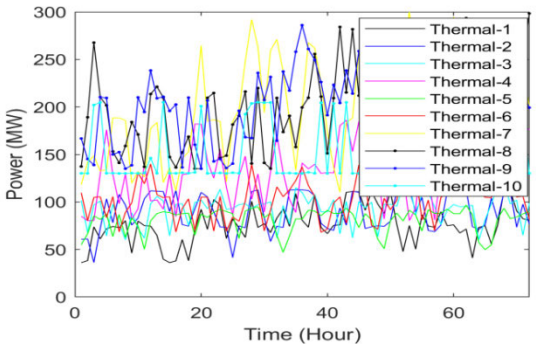

FIGURE 12. Power Generation received from thermal unit with DSM using HPSO-TVAC.

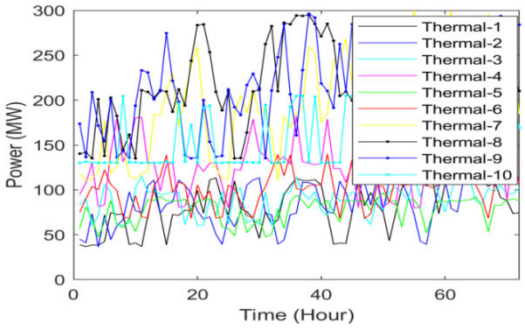

FIGURE 13. Power Generation received from thermal unit without DSM using HPSO-TVAC.

Figure 14 depicts the variation of power generation in MW with time (in hours), which corresponds to the best cost obtained from four hydropower plants: one WTG, one solar plant, and one PSH plant using HPSO-TVAC with DSM and with fuel constraints over a 72-hour period.

Figure 15 depicts the variation of power generation in MW with time (in hours), corresponding to the best cost obtained from four hydropower plants, one WTG, one solar plant, and one PSH plant using HPSO-TVAC with DSM and no fuel constraints over a 72-hour period.

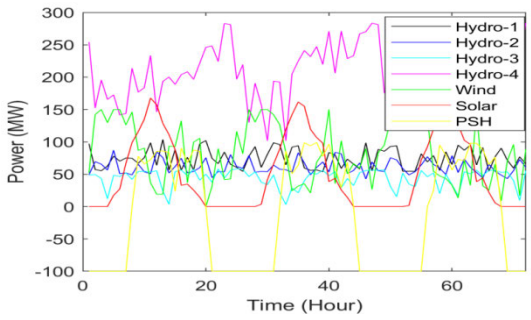

FIGURE 14. Power Generation received from different plants with DSM and fuel constraints using HPSO-TVAC.

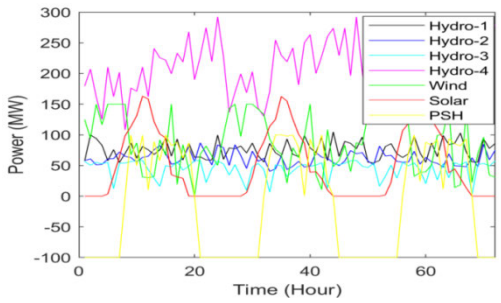

FIGURE 15. Power Generation received from different plants with DSM using HPSO-TVAC.

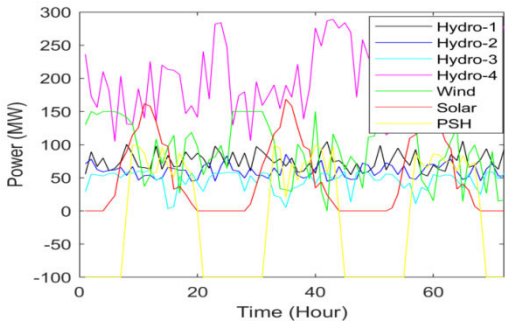

FIGURE 16. Power generation obtained from hydro plants, WTG, solar PV plant and PSH without DSM using HPSO-TVAC.

Figure 16 shows the variation of power generation in MW with time (in hours), corresponding to the best cost obtained from four hydropower plants: one WTG, one solar plant, and one PSH plant using HPSO-TVAC without DSM and without fuel constraints for a time span of 72 hr.

The variation shown in Fig. 17 for power generation in MW versus time (in hours) corresponds to the best cost obtained from ten thermal generating units using GWO while accounting for DSM and fuel constraints over a 72-hour period.

The variation shown in Fig. 18 for power generation in MW versus time in hours corresponds to the best cost obtained from ten thermal generating units using GWO with DSM and no fuel constraints over a 72-hour period.

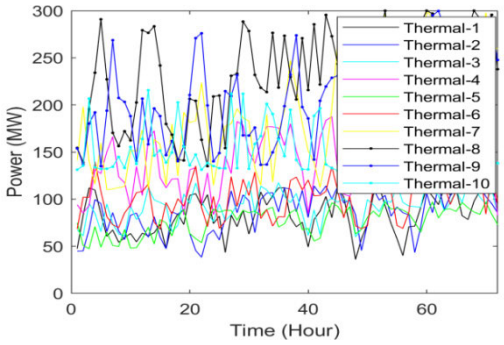

FIGURE 17. Power Generation received from thermal unit with DSM and fuel constraints using GWO.

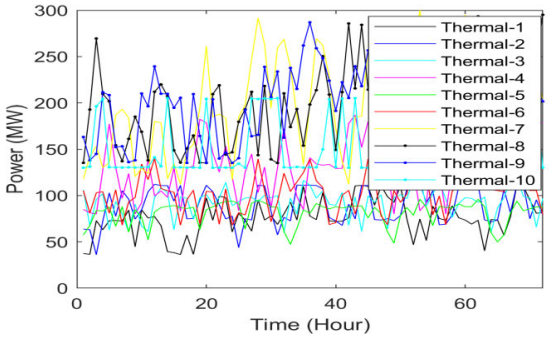

FIGURE 18. Power Generation received from thermal units with DSM using GWO.

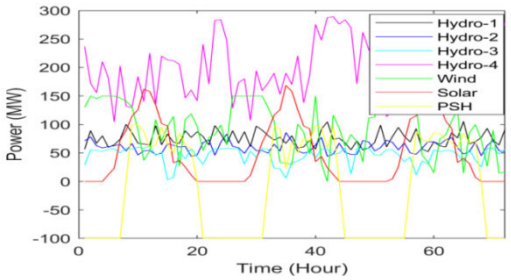

FIGURE 19. Power Generation received different plants with DSM and fuel constraints using GWO.

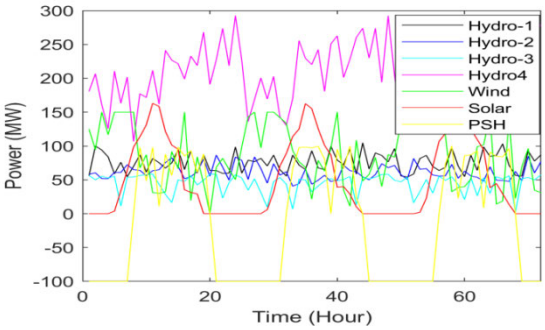

FIGURE 20. Power Generation received from different plants with DSM using GWO.

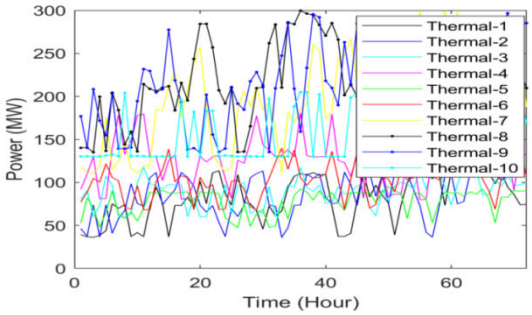

FIGURE 21. Power Generation received from thermal units without DSM using GWO.

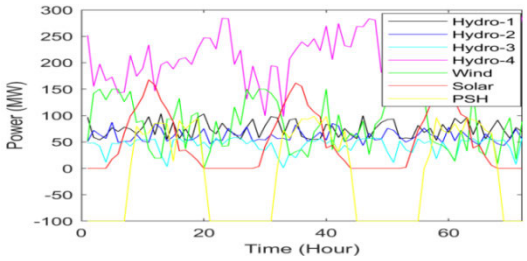

FIGURE 22. Power Generation received from different plants without DSM using GWO.

The variation shown in Fig. 19 for power generation in MW with time (in hours) corresponds to the best cost obtained from four hydropower plants: one WTG, one solar plant, and one PSH plant using GWO, considering DSM and fuel constraints for a time span of 72 hr.

Figure 20 shows the variation of power generation in MW with time in hours, corresponding to the best cost obtained from four hydropower plants, one WTG, one solar plant, and one PSH plant, using GWO with DSM and without fuel constraints for a time span of 72 hr.

The variation in power generation in MW with time in hours shown in Fig. 21 corresponds to the best cost obtained from ten thermal generating units using GWO without DSM and without fuel constraints over a 72-hour period.

Figure 22 depicts the variation of power generation in MW with time in hours, which corresponds to the best cost obtained from four hydropower plants, one WTG, one solar plant, and one PSH plant, all using GWO without DSM and without fuel constraints over a 72-hour period.

Figure 23 shows the amount of fuel per ton being supplied with fuel based on the best cost gained from the planned ECO for ten thermal generators at different intervals.

Figure 24 depicts the fuel supply in tons based on the best cost obtained from the planned HPSO-TVAC for ten thermal generators at different 18-hour intervals. Each interval contains 4 hours when considering DSM.

Figure 25 shows the amount of fuel, in tons, being supplied based on the best cost gained from the planned GWO to

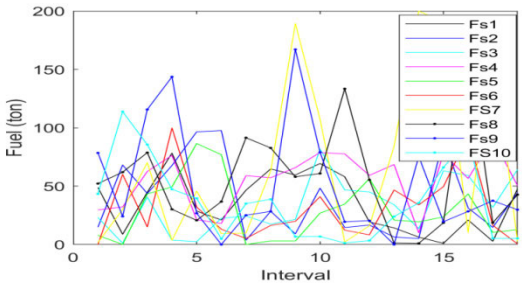

FIGURE 23. Fuel delivered to thermal units using ECO.

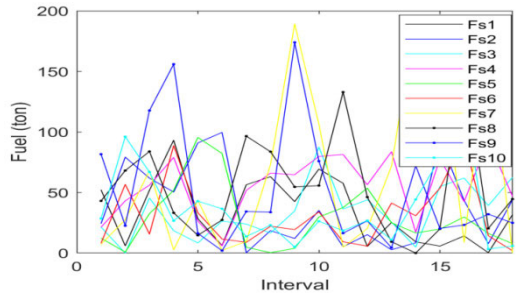

FIGURE 24. Fuel delivered to thermal generators using HPSO-TVAC.

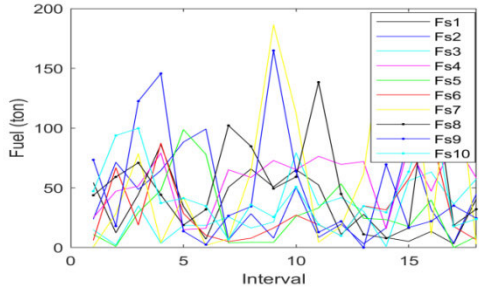

FIGURE 25. Fuel delivered to thermal units using GWO.

ten thermal generators at different 18-hour intervals. Each interval contains 4 hours when considering DSM.

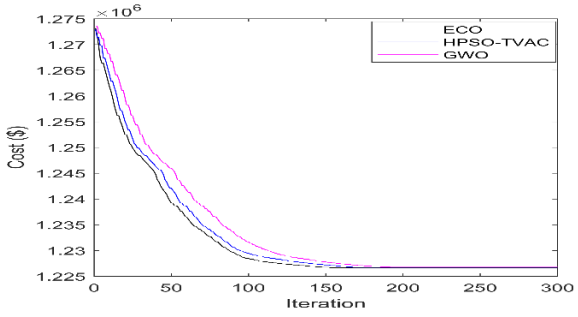

FIGURE 26. Characteristics of cost convergence with DSM and fuel constraints.

Characteristics of cost convergence obtained from ECO, HPSO-TVAC, and GWO considering DSM and fuel limits are shown in Fig. 26. From the above curve, it is observed that ECO converges in 153 iterations. HPSO-TVAC converges in 168 iterations, and GWO converges in 192 iterations. As a result, the authors can conclude that ECO is faster than HPSO-TVAC, while HPSO-TVAC is faster than GWO. Hence, the performance of ECO is the best among all other techniques.

Cost convergence characteristics are depicted in Figs. 25 and 26 by considering DSM and taking into account ECO, HPSO-TVAC, and GWO.

Characteristics of cost convergence obtained from ECO, HPSO-TVAC, and GWO with and without fuel limits are shown in Fig. 27. From the above curve, it is observed that ECO converges after 173 iterations. HPSO-TVAC converges in 180 iterations, and GWO converges in 189 iterations. From this, it can be concluded that ECO converges faster than HPSO-TVAC, while HPSO-TVAC converges faster than GWO. Hence, the performance of ECO is the best among all other techniques.

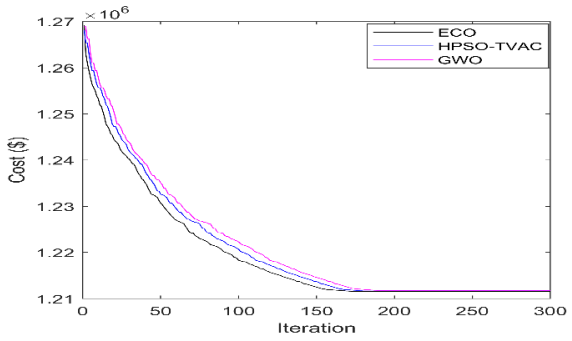

FIGURE 27. Characteristics of cost convergence with DSM.

Characteristics of cost convergence obtained from ECO, HPSO-TVAC, and GWO without DSM and without fuel limits are shown in Fig. 28. From the above curve, it is observed that ECO converges after 177 iterations. HPSO-TVAC converges in 185 iterations, and GWO converges in 196 iterations. From this, it can be concluded that ECO converges faster than HPSO-TVAC, while HPSO-TVAC converges faster than GWO. Hence, the performance of ECO is the best among all other methods.

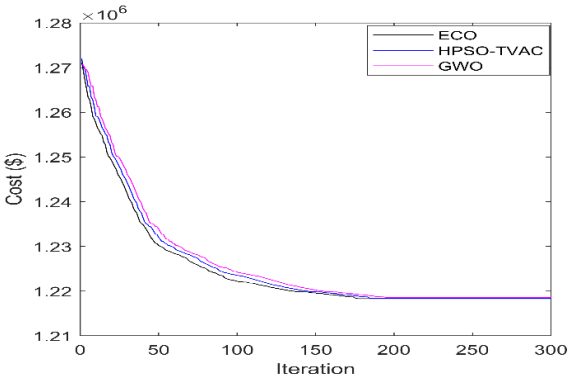

FIGURE 28. Characteristics of cost convergence without DSM.

Table 5 shows the overall comparison, taking three different cases. The three cases are: (a) with DSM and

TABLE 5. Performance comparison.

		Best cost ($)	Average cost ($)	Worst cost ($)	CPU time (s)
With DSM and with fuel constraints	ECO	1226644	1226648	1226655	123.74
	HPSO-TVAC	1226717	1226725	1226736	128.83
	GWO	1226774	1226786	1226799	129.05
With DSM and without fuel constraints	ECO	1211571	1211574	1211579	104.65
	HPSO-TVAC	1211665	1211671	1211679	108.66
	GWO	1211795	1211805	1211817	106.89
Without DSM and without fuel constraints	ECO	1218311	1218315	1218320	102.35
	HPSO-TVAC	1218421	1218426	1218433	106.55
	GWO	1218542	1218551	1218561	104.79

fuel constraints (b) With DSM and without fuel constraints; (c) Without DSM and without fuel constraints among the different optimization techniques on the basis of best cost, average cost, worst cost dollars, and CPU time in seconds. In all of the above cases, ECO was the least expensive technique when compared to HPSO, TVAC, and GWO. It is also observed that the cost is lowest in the second case, i.e., with DSM and without fuel constraints. In all three of the cases above, the CPU time is lower with ECO compared to HPSO-TVAC and GWO. Again, it is least in the third case, i.e., without DSM and without fuel constraints, as compared to the other two cases. Even if fuel limitations are ignored, the cost of using DSM is less than the cost of not using it. This table further shows that the cost obtained from the suggested ECO is the cheapest of the three approaches.

2) DISCUSSION

Loading of thermal units without considering fuel constraints depends on ramp rate limits, generation limits, and fuel cost coefficients. Loading of thermal units with fuel constraints is determined not only by generation limits, ramp rate limits, and fuel cost coefficients but also by fuel consumption coefficients, fuel delivery limits, fuel storage limits, and thermal unit initial fuel storage. The power generated by the thermal unit is never used to dispatch power economically.

V. CONCLUSION

In this work, ECO is proposed for solving complex fuel-constrained short-term hydrothermal scheduling involving thermal generators, cascaded hydro power plants, solar, WTGs, and PSH plants with and without DSM for three different scenarios. Three scenarios are considered here: (a) with DSM and fuel constraints; (b) with DSM and no fuel constraints; and (c) without DSM and no fuel constraints. The test system is also solved by using the HPSO-TVAC and GWO. In the case of DSM and fuel constraints, ECO is nearly 0.00595% less expensive than HPSO-TVAC and nearly 0.0001% less expensive than GWO. In the case of DSM and without fuel constraints, ECO provides nearly 0.00776% less cost compared to HPSO-TVAC and nearly 0.0001% less cost compared to GWO. In the absence of DSM and fuel constraints, ECO is nearly 0.0090% less expensive than HPSO-TVAC and nearly 0.0189% less expensive than GWO. Likewise, considering CPU time, in the case of DSM and with fuel constraints, ECO is using 3.95% less time compared to HPSO-TVAC and nearly 4.11% less time compared to GWO. In cases with and without fuel constraints, ECO has 3.69% and 2.09% less CPU time compared to HPSO-TVAC and GWO, respectively. In the absence of DSM and without fuel constraints, ECO provides nearly 4.1% and 2.33% less CPU time compared to HPSO-TVAC and GWO, respectively. After analysis, it is concluded that the proposed ECO provides better results than HPSO-TVAC and GWO.

REFERENCES

[1] F. J. Trefny and K. Y. Lee, "Economic fuel dispatch," *IEEE Trans. Power App. Syst.*, vol. PAS-100, no. 7, pp. 3468–3477, Jul. 1981.
[2] A. B. R. Kumar, D. F. Hackett, J. Eisenhauer, S. Vemuri, and R. Lugtu, "Fuel resource scheduling, Part I—Overview of an energy management problem," *IEEE Trans. Power App. Syst.*, vol. PAS-103, no. 7, pp. 1542–1548, Jul. 1984.
[3] A. B. R. Kumar and S. Vemuri, "Fuel resource scheduling, Part-II—Contrained economic dispatch," *IEEE Trans. Power App. Syst.*, vol. PAS-103, no. 7, pp. 1549–1555, Jul. 1984.
[4] A. G. Bakirtzis and E. S. Gavanidou, "Optimum operation of a small autonomous system with unconventional energy sources," *Electric Power Syst. Res.*, vol. 23, no. 2, pp. 93–102, Mar. 1992.
[5] N. A. Khan, A. B. Awan, A. Mahmood, S. Razzaq, A. Zafar, and G. A. S. Sidhu, "A Combined emission economic dispatch of power system including solar photo voltaic generation," *Energy Convers. Manag.*, vol. 92, no. 1, pp. 82–91, 2015.
[6] B. P. Cotia, C. L. T. Borges, and A. L. Diniz, "Optimization of wind power generation to minimize operation costs in the daily scheduling of hydrothermal systems," *Int. J. Electr. Power Energy Syst.*, vol. 113, pp. 539–548, Dec. 2019.
[7] J. I. Perez-Diaz and J. Jimenez, "Contribution of a pumped-storage hydropower plant to reduce the scheduling costs of an isolated power system with high wind power penetration," *Energy*, vol. 109, no. 1, pp. 92–104, 2016.
[8] S. Fadil and B. Urazel, "Solution to security-constrained non-convex pumped-storage hydraulic unit scheduling problem by modified subgradient algorithm based on feasible values and pseudo water price," *Electric Power Compon. Syst.*, vol. 41, no. 2, pp. 111–135, Jan. 2013.
[9] S. K. Khandualo, A. K. Barisal, and P. K. Hota, "Scheduling of pumped storage hydrothermal system with evolutionary programming," *J. Clean Energy Technol.*, vol. 1, no. 4, pp. 308–312, 2013.

[10] A. Helseth, A. Gjelsvik, B. Mo, and Ú. Linnet, "A model for optimal scheduling of hydro thermal systems including pumped-storage and wind power," *IET Gener., Transmiss. Distrib.*, vol. 7, no. 12, pp. 1426–1434, Dec. 2013.
[11] T. Ma, H. Yang, L. Lu, and J. Peng, "Pumped storage-based standalone photovoltaic power generation system: Modeling and techno-economic optimization," *Appl. Energy*, vol. 137, pp. 649–659, Jan. 2015.
[12] R. S. Patwal, N. Narang, and H. Garg, "A novel TVAC-PSO based mutation strategies algorithm for generation scheduling of pumped storage hydrothermal system incorporating solar units," *Energy*, vol. 142, pp. 822–837, Jan. 2018.
[13] T. T. Nguyen, D. N. Vo, and B. H. Dinh, "An effectively adaptive selective cuckoo search algorithm for solving three complicated short-term hydrothermal scheduling problems," *Energy*, vol. 155, pp. 930–956, Jul. 2018.
[14] J. Jian, S. Pan, and L. Yang, "Solution for short-term hydrothermal scheduling with a logarithmic size mixed-integer linear programming formulation," *Energy*, vol. 171, pp. 770–784, Mar. 2019.
[15] H. Yin, F. Wu, X. Meng, Y. Lin, J. Fan, and A. Meng, "Crisscross optimization based short-term hydrothermal generation scheduling with cascaded reservoirs," *Energy*, vol. 203, Jul. 2020, Art. no. 117822.
[16] M. Kaur, J. S. Dhillon, and D. P. Kothari, "Crisscross differential evolution algorithm for constrained hydrothermal scheduling," *Appl. Soft Comput.*, vol. 93, Aug. 2020, Art. no. 106393.
[17] W. Hou, H. Wei, and R. Zhu, "Data-driven multi-time scale robust scheduling framework of hydrothermal power system considering cascade hydropower station and wind penetration," *IET Gener., Transmiss. Distrib.*, vol. 13, no. 6, pp. 896–904, Mar. 2019.
[18] V. P. Sakthivel, K. Thirumal, and P. D. Sathya, "Short term scheduling of hydrothermal power systems with photovoltaic and pumped storage plants using quasi-oppositional turbulent water flow optimization," *Renew. Energy*, vol. 191, pp. 459–492, May 2022.
[19] V. P. Sakthivel, K. Thirumal, and P. D. Sathya, "Quasi-oppositional turbulent water flow-based optimization for cascaded short term hydrothermal scheduling with valve-point effects and multiple fuels," *Energy*, vol. 251, Jul. 2022, Art. no. 123905.
[20] A. Yousefi, H. H.-C. Iu, T. Fernando, and H. Trinh, "An approach for wind power integration using demand side resources," *IEEE Trans. Sustain. Energy*, vol. 4, no. 4, pp. 917–924, Oct. 2013.
[21] A. Mehdizadeh and N. Taghizadegan, "Robust optimisation approach for bidding strategy of renewable generation-based microgrid under demand side management," *IET Renew. Power Gener.*, vol. 11, no. 11, pp. 1446–1455, Sep. 2017.
[22] J. Hetzer, D. C. Yu, and K. Bhattarai, "An economic dispatch model incorporating wind power," *IEEE Trans. Energy Convers.*, vol. 23, no. 2, pp. 603–611, Jun. 2008.
[23] R. H. Liang and J. H. Liao, "A fuzzy-optimization approach for generation scheduling with wind and solar energy systems," *IEEE Trans. Power Syst.*, vol. 22, no. 4, pp. 1665–1674, Nov. 2007.
[24] P. Giorsetto and K. Utsurogi, "Development of a new procedure for reliability modeling of wind turbine generators," *IEEE Trans. Power App. Syst.*, vol. PAS-102, no. 1, pp. 134–143, Jan. 1983.
[25] C. Shilaja and K. Ravi, "Optimization of emission/economic dispatch using Euclidean affine flower pollination algorithm (eFPA) and binary FPA (BFPA) in solar photo voltaic generation," *Renew. Energy*, vol. 107, pp. 550–566, Jul. 2017.
[26] X. Feng, Y. Wang, H. Yu, and F. Luo, "A novel intelligence algorithm based on the social group optimization behaviors," *IEEE Trans. Syst., Man, Cybern., Syst.*, vol. 48, no. 1, pp. 65–76, Jan. 2018.
[27] C. E. Shannon, "A mathematical theory of communication," *Bell Syst. Tech. J.*, vol. 27, no. 3, pp. 379–423, Jul. 1948.
[28] L. Lakshminarasimman and S. Subramanian, "Short-term scheduling of hydrothermal power system with cascaded reservoirs by using modified differential evolution," *IEE Proc.-Gener., Transmiss. Distrib.*, vol. 153, no. 6, pp. 693–700, 2006.
[29] D. C. Walters and G. B. Sheble, "Genetic algorithm solution of economic dispatch with valve point loading," *IEEE Trans. Power Syst.*, vol. 8, no. 3, pp. 1325–1332, Aug. 1993.
[30] M. Jafari, E. Salajegheh, and J. Salajegheh, "Elephant clan optimization: A nature-inspired metaheuristic algorithm for the optimal design of structures," *Appl. Soft Comput.*, vol. 113, Dec. 2021, Art. no. 107892, doi: 10.1016/j.asoc.2021.107892.
[31] A. Ratnaweera, S. K. Halgamuge, and H. C. Watson, "Self-organizing hierarchical particle swarm optimizer with time-varying acceleration coefficients," *IEEE Trans. Evol. Comput.*, vol. 8, no. 3, pp. 240–255, Jun. 2004.
[32] S. Mirjalili, S. M. Mirjalili, and A. Lewis, "Grey wolf optimizer," *Adv. Eng. Softw.*, vol. 69, pp. 46–61, Mar. 2014.

CHITRALEKHA JENA received the B.Tech. degree in electrical engineering from the College of Engineering and Technology, Odisha University of Agriculture and Technology (OUAT), Bhubaneswar, India, in 2001, the M.Tech. degree from KIIT University, Bhubaneswar, in 2009, and the D.Phil. degree from Jadavpur University, Kolkata, India, in 2017. She is currently with the School of Electrical Engineering, KIIT University. She has published more than 40 research papers in different peer-reviewed journals and conferences. Her research interests include power system restructuring, power system planning, smart grid technologies, meta-heuristic optimization techniques, reliability analysis of renewable energy systems, power quality analysis, and renewable energy integration.

MOUSUMI BASU received the Ph.D. degree from Jadavpur University, Kolkata, India. She is currently working as a Professor with the Department of Power Engineering, Jadavpur University. She has published more than 100 research papers in reputed international journals and conferences. Her research interests include power system optimization, renewable energy, and soft computing technique.

JOSEP M. GUERRERO (Fellow, IEEE) received the B.S. degree in telecommunications engineering, the M.S. degree in electronics engineering, and the Ph.D. degree in power electronics from the Technical University of Catalonia, Barcelona, in 1997, 2000, and 2003, respectively. Since 2011, he has been a Full Professor with the Department of Energy Technology, Aalborg University, Denmark, where he is responsible for the Microgrid Research Program. Since 2014, he has been the Chair Professor with Shandong University. Since 2015, he has been a Distinguished Guest Professor with Hunan University. Since 2016, he has also been a Visiting Professor Fellow with Aston University, U.K., and a Guest Professor with the Nanjing University of Posts and Telecommunications. Since 2019, he became a Villum Investigator by The Villum Fonden, which supports the Center for Research on Microgrids (CROM), Aalborg University, being he has the Founder and the Director of the CROM (www.crom.et.aau.dk). He has published more than 600 journal articles in the fields of microgrids and renewable energy systems, which are cited more than 50 000 times. His research interests include different microgrid aspects, including power electronics, distributed energy-storage systems, hierarchical and cooperative control, energy management systems, smart metering, and the Internet of Things for ac/dc microgrid clusters and islanded minigrids. Specially focused on microgrid technologies applied to offshore wind, maritime microgrids for electrical ships, vessels, ferries and seaports, and space microgrids applied to nanosatellites and spacecrafts. In 2015, he was elevated as a IEEE Fellow for his contributions on distributed power systems and microgrids. He received the Best Paper Award of the IEEE TRANSACTIONS ON ENERGY CONVERSION, from 2014 to 2015, and the Best Paper Prize of IEEE-PES, in 2015. As well, he received the Best Paper Award of the *Journal of Power Electronics*, in 2016. During six consecutive years, from 2014 to 2019, he was awarded by Clarivate Analytics (former Thomson Reuters) as a Highly Cited Researcher with 50 highly cited papers. He is currently an associate editor for a number of IEEE TRANSACTIONS.

ABDULLAH ABUSORRAH (Senior Member, IEEE) is currently with the Center of Research Excellence in Renewable Energy and Power Systems, Department of Electrical and Computer Engineering, Faculty of Engineering, K. A. CARE Energy Research and Innovation Center, King Abdulaziz University, Jeddah, Saudi Arabia. His research interests include power system restructuring, power system planning, smart grid technologies, meta-heuristic optimization techniques, reliability analysis of renewable energy systems, power quality analysis, and renewable energy integration.

YUSUF AL-TURKI is currently with the Center of Research Excellence in Renewable Energy and Power Systems, Department of Electrical and Computer Engineering, Faculty of Engineering, K. A. CARE Energy Research and Innovation Center, King Abdulaziz University, Jeddah, Saudi Arabia. His research interests include power system restructuring, power system planning, smart grid technologies, meta-heuristic optimization techniques, reliability analysis of renewable energy systems, power quality analysis, and renewable energy integration.

BASEEM KHAN (Senior Member, IEEE) received the B.Eng. degree in electrical engineering from Rajiv Gandhi Technological University, Bhopal, India, in 2008, and the M.Tech. and Ph.D. degrees in electrical engineering from the Maulana Azad National Institute of Technology, Bhopal, in 2010 and 2014, respectively. He is currently working as a Faculty Member with Hawassa University, Ethiopia. He has published more than 100 research papers in well reputable research journals, including IEEE TRANSACTIONS, IEEE ACCESS, *Computers and Electrical Engineering* (Elsevier), *IET Generation, Transmission & Distribution* (GTD), *IET Renewable Power Generation* (RPG), and *IET Power Electronics*. Furthermore, he has published, authored, and edited books with Wiley, CRC Press, and Elsevier. His research interests include power system restructuring, power system planning, smart grid technologies, meta-heuristic optimization techniques, reliability analysis of renewable energy systems, power quality analysis, and renewable energy integration.

ANDREA JUSTO is currently with the Center for Research on Microgrids (CROM), AAU Energy, Aalborg University, Denmark. Her research interests include power system restructuring, power system planning, smart grid technologies, meta-heuristic optimization techniques, reliability analysis of renewable energy systems, power quality analysis, and renewable energy integration.

ARJYADHARA PRADHAN received the M.Tech. degree in solar PV system with the focus on maximum power point tracking and the Ph.D. degree from KIIT University, Bhubaneshwar, Odisha. She is currently working as an Assistant Professor with the School of Electrical Engineering, KIIT University. She has guided five M.Tech. students and 25 B.Tech. students. She has published 15 papers both in international and national journals. She has also published papers in 35 international and national conferences and among them six of IEEE conference. Her broad working area is solar photovolatics and renewable energy systems. She is a Life Member of various professional bodies, such as SESI, IE, ISTE, ISLE, and ISC. She was awarded with the Institutional Award for best paper from the Institution of Engineers, Odisha, and the Emerging Scientist Award from VDGOOD Technology Factory International Scientist Awards on Engineering, Science and Medicine, Visakhapatnam, India, in December 2021. She was also awarded with the Best Faculty by Education Expo TV and the Best Research Award by Science Father, in 2021, for her valuable contributions in the field of teaching, learning, and research.